Vacuum consolidation and its combination with embankment loading

J.-C. Chai, J.P. Carter, and S. Hayashi

Abstract: A method is proposed for determining the optimum penetration depth of prefabricated vertical drains (PVDs) in cases where vacuum consolidation is combined with the use of PVDs in a clayey deposit with two-way drainage. The advantages of combining vacuum pressure with embankment loading are discussed in terms of reducing preloading-induced lateral displacement of the subsoil, increasing the effective surcharge loading, and reducing construction time in the case of road construction. A vacuum consolidation project conducted in Saga, Japan, is described, and the results from a fully instrumented test section are presented and analyzed using a two-dimensional finite element approach. The numerical simulations compare well with the field measurements. The validated numerical approach is then used to examine the response of soft subsoil subjected to vacuum consolidation. The results confirm the usefulness of the proposed method for determining the optimum penetration depth of PVDs and the advantages of combining vacuum pressure with embankment loading.

Key words: vacuum consolidation, preloading, prefabricated vertical drain, FEM analysis, embankment.

Résumé : On propose une méthode pour déterminer la profondeur de pénétration optimale de drains verticaux préfabriqués (PVD) dans les cas où la consolidation par le vide est combinée avec l'utilisation de PVD dans uin dépôt d'argile avec drainage dans les deux directions. On discute les avantage de combiner la pression de vide avec le chargement du remblai en termes de réduction du déplacement latéral du sous-sol induit par le préchargement, l'augmentation effective de la surcharge, et la réduction du temps de construction dans le cas de construction de routes. On décrit un projet de consolidation par le vide réalisé à Saga, Japon; on présente les résultats d'une section d'essai complètement instrumentée et on l'analyse au moyen d'une approche en éléments finis à deux dimensions. Les simulations numériques se comparent bien avec les mesures sur le terrain. On a alors utilisé l'approche numérique validée pour examiner la réponse d'un sous-sol mou soumis à une consolidation par le vide. Les résultats confirment l'utilité de la méthode proposée pour déterminer la profondeur de pénétration optimale des PVD et l'avantage de combiner la pression de vide avec le chargement du remblai.

Mots clés : consolidation par le vide, préchargement, drain vertical préfabriqué, analyse en éléments finis, remblai.

[Traduit par la Rédaction]

Introduction

Vacuum consolidation, originally developed by Kjellman (1952), has been widely used to improve soft clayey deposits (e.g., Tang and Shang 2000; Tran et al. 2004). Consolidating soft clayey deposits by applying a vacuum pressure has several advantages over embankment loading, e.g., no fill material is required, construction periods are generally shorter, and there is no need for heavy machinery. In addition, the vacuum consolidation method does not put any chemical ad-

mixtures into the ground and consequently is an environmentally friendly ground improvement method.

Chai et al. (2005a, 2005b) discussed the characteristics of vacuum consolidation. One characteristic is the effect of the drainage boundary conditions of the soil deposit on the consolidation. The settlement induced by vacuum pressure for a deposit with two-way drainage is less than that for a deposit with one-way drainage. In engineering practice, vacuum consolidation is generally combined with prefabricated vertical drains (PVDs) to accelerate the consolidation process. In the case of a clayey deposit underlain by a more permeable layer, e.g., a sand or gravel layer, two-way drainage conditions are likely to apply. To avoid vacuum pressure losses into the sand or gravel layer via the PVDs, normally the PVDs are installed so that they only partially penetrate the clayey layer. There is no theoretical guide for determining the penetration depth of the PVDs at which the optimum vacuum consolidation is achieved, however.

A particular disadvantage of vacuum consolidation is that it may cause cracks in the surrounding surface area due to inward lateral displacement of the ground induced by application of the vacuum pressure. Furthermore, the magnitude of the applied vacuum pressure is limited by atmospheric pressure (about 100 kPa). Therefore, in some cases, the

J.-C. Chai.[1] Department of Civil Engineering, Saga University, 1 Honjo, Saga 840-8502, Japan.
J.P. Carter.[2] Department of Civil Engineering, The University of Sydney, Sydney, NSW 2006, Australia.
S. Hayashi. Institute of Lowland Technology, Saga University, 1 Honjo, Saga 840-8502, Japan.

[1]Corresponding author (e-mail: chai@cc.saga-u.ac.jp).
[2]Present address: Faculty of Engineering and Built Environment, The University of Newcastle, Callaghan, NSW 2308, Australia.

combination of vacuum pressure and embankment loading may provide better overall ground improvement (Bergado et al. 1998; Tran et al. 2004).

In this paper, a method for determining the optimum penetration depth of PVDs in cases of two-way drainage of a clayey deposit and the advantages of combining vacuum pressure with embankment loading are discussed. A field vacuum consolidation project conducted in Saga, Japan, is subsequently described. Ground behaviour at the test section was simulated by the finite element method (FEM), and a comparison of the simulations and the field test results is provided. Lastly, ground conditions similar to those at the Saga test section have been adopted in a theoretical study that illustrates the effects on the subsoil response of the PVD penetration depth and various combinations of vacuum pressure and embankment loading.

Optimum PVD penetration depth

In field vacuum consolidation projects, generally the vacuum pressure is applied at the ground surface so that the final vacuum pressure distribution in the ground depends on the properties and drainage boundary condition of the deposit. Considering a one-dimensional (1D) problem and a uniform soil deposit, if the bottom boundary is not drained, the final vacuum pressure in the deposit will be uniform. Conversely, if drainage can occur through the bottom boundary such that a vacuum pressure cannot be effectively maintained at this boundary, the vacuum pressure distribution at the end of vacuum consolidation, i.e., when a steady-state distribution of suction (excess) pore pressure is established throughout the soil deposit, will be linear, with the maximum value at the ground surface and a value of zero at the bottom (Chai et al. 2005a), which involves steady upward water flow through the clayey layer. In the case of a non-uniform deposit, the vacuum pressure distribution within the deposit will depend on the relative values of the hydraulic conductivities of the individual layers. For steady upward water flow in a layered deposit, the following condition must be satisfied to maintain continuity of the flow:

$$[1] \qquad i_1 k_{v1} = i_2 k_{v2} = \ldots = i_i k_{vi}$$

where i_i and k_{vi} are the hydraulic gradient and hydraulic conductivity of the ith layer, respectively. A layer with a lower value of k must have a higher value of i, and a higher i value implies a larger variation of vacuum pressure within the layer.

For a clayey deposit with two-way drainage and partially improved (penetrated) by PVDs, the possible vacuum pressure distribution within the layers at the end of vacuum consolidation is illustrated in Fig. 1. The optimum penetration depth is the depth at which the clay layer will exhibit the largest consolidation settlement under a given vacuum pressure applied at the surface. Assuming that the static water table is at the ground surface, the k values are uniform in both the PVD-improved zone and the unimproved zone, and at the end of vacuum consolidation the vacuum pressure is p_{v0} at the ground surface and p_{v1} at the base of the PVD-improved zone (Fig. 1), then the flow continuity requires

Fig. 1. Illustration of vacuum consolidation with PVD improvement: (a) soil profile, drained and with vacuum pressure applied; (b) vacuum pressure distribution.
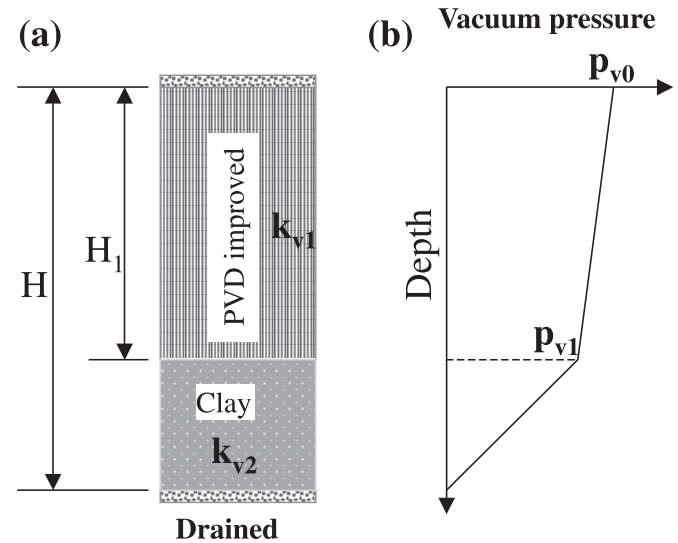
$$[2] \qquad k_{v1} \frac{p_{v0} - p_{v1}}{H_1} = k_{v2} \frac{p_{v1}}{H - H_1}$$

where k_{v1} and k_{v2} are the vertical hydraulic conductivities of layers 1 and 2, respectively; H_1 is the thickness of the PVD-improved zone; and H is the thickness of the soft clayey deposit. If the integration of vacuum pressure with depth is denoted by A, it can be shown that A is expressed as

$$[3] \qquad A = [p_{v0} H_1] - \left[\frac{1}{2}(p_{v0} - p_{v1})H_1 \right] + \left[\frac{1}{2}(H - H_1)p_{v1} \right]$$

Substituting eq. [2] into eq. [3] to eliminate p_{v1}, an expression for A is obtained as follows:

$$[4] \qquad A = \frac{1}{2} p_{v0}(H_1 + H) - \frac{1}{2} H \frac{p_{v0} k_{v2} H_1}{k_{v1} H - (k_{v1} - k_{v2})H_1}$$

Differentiating A with respect to H_1 and equating this to zero provides an expression for the optimum penetration depth H_1 as follows:

$$[5] \qquad H_1 = \left(\frac{k_{v1} - \sqrt{k_{v1} k_{v2}}}{k_{v1} - k_{v2}} \right) H$$

Chai et al. (2001) proposed a method to calculate the equivalent vertical hydraulic conductivity of PVD-improved subsoil, which can be used to evaluate the value of k_{v1}, i.e., the mass vertical hydraulic conductivity of the PVD-improved zone:

$$[6] \qquad k_{v1} = \left(1 + \frac{2.5 l^2}{\mu D_e^2} \frac{k_h}{k_v} \right) k_v$$

where D_e is the diameter of a unit cell (containing a PVD and its improvement area); k_h and k_v are the horizontal and vertical hydraulic conductivities of the natural soil, respectively; and $l (= H_1)$ is the drainage length of the PVDs. The

parameter μ represents the effects of spacing, smear, and the well resistance of the PVDs, which can be expressed as follows (Hansbo 1981):

$$[7] \qquad \mu = \ln\left(\frac{n}{s}\right) + \frac{k_h}{k_s}\ln(s) - \frac{3}{4} + \pi\frac{2l^2k_h}{3q_w}$$

where $n = D_e/d_w$ (d_w is the diameter of the drain), $s = d_s/d_w$ (d_s is the diameter of the smear zone), k_s is the hydraulic conductivity of the smear zone, and q_w is the the discharge capacity of the PVDs. Since H_1 in eq. [5] and l in eqs. [6] and [7] have the same meaning, some iteration is needed to obtain the value of H_1. Also note that if the value of k_{v1} in the PVD-improved zone or k_{v2} in the unimproved zone is not uniform, an equivalent hydraulic conductivity (k_{eq}) can be used, but using eq. [5] may not yield an exact optimum penetration depth. For a two-layer case, k_{eq} can be calculated as follows:

$$[8] \qquad k_{eq} = \frac{k_{i1}k_{i2}H_i}{k_{i1}H_{i2} + k_{i2}H_{i1}}$$

where H_i is the thickness of the PVD-improved or unimproved zone; H_{i1} and H_{i2} are the thicknesses of sublayers 1 and 2 in H_i, respectively; and k_{i1} and k_{i2} are the hydraulic conductivities of sublayers 1 and 2 in H_i, respectively. Furthermore, if the compressibility of the soil around the base of the PVD-improved zone varies significantly, from a settlement point of view, eq. [5] may not guarantee the optimum penetration depth.

Note that the method proposed here also has the following limitations:

(1) The effect of horizontal water flow from the surrounding area into the zone of soil improved by vacuum consolidation is not considered.

(2) Only the condition at the end of vacuum consolidation is considered, i.e., when a steady-state distribution of suction (excess) pore pressure is established throughout the soil deposit. The effect of the PVD installation depth on the consolidation process is not considered.

(3) By contrast, in eq. [5], the initial thickness of the soft deposit is used to calculate the initial PVD penetration depth. If the whole deposit compresses uniformly, these contradictory conditions may not cause any significant error, but if the upper soil layer compresses much more than the lower layer, some error may be introduced.

Benefits of combining vacuum pressure with embankment load

The advantages of combining vacuum pressure with embankment load can be discussed in terms of preloading pressure, construction time, and lateral deformation of the ground.

Preloading pressure

Theoretically, the maximum vacuum pressure that may be applied is 1 atm (about 100 kPa), but practically achievable values are normally in the range from 60 to 80 kPa (Bergado et al. 1998; Tang and Shang 2000). In cases where the required preloading pressure is greater than about 60–80 kPa, application of a vacuum pressure alone cannot satisfy the preloading requirement, and combining vacuum pressure

with embankment loading can be used to solve the problem. Adopting a preloading pressure greater than the permanent structural load can also eliminate or reduce residual settlements after the structure is constructed.

Construction time

Most soft clayey deposits are found in lowland regions. After vacuum preloading, the surface elevation of the treated area will be generally lower than that of the surrounding area. For road, railway, airport runway, and other civil engineering structures, an embankment will usually have to be constructed on the improved ground. Constructing the embankment during the preloading period not only increases the preloading pressure but also should save construction time for the whole project.

Lateral deformation

Embankment loading will cause both settlement of the underlying soft subsoil and generally outward lateral displacement. This lateral displacement is mainly caused by the shear stresses induced by the embankment load, and if these shear stresses are large enough in some regions of the subsoil, they will cause shear failure within those regions. By contrast, the vacuum pressure technique tends to apply an isotropic incremental consolidation pressure to the soft subsoil, which will induce settlement and inward lateral displacement. The inward deformation may cause some surface cracks around the preloading area.

In situations where existing structures are adjacent to the preloading area, both outward lateral movement of the treated area induced by embankment loading and inward lateral deformation induced by vacuum pressure are undesirable. To avoid or minimize lateral deformations during the preloading period, it is possible to combine embankment loading with application of a vacuum pressure (Bergado et al. 1998; Tran et al. 2004).

In the following sections, a vacuum consolidation project in Saga, Japan, is described and analyzed to illustrate the effect of PVD penetration depth on the settlement induced by vacuum consolidation and the advantages of the combination of embankment load with vacuum pressure.

Vacuum consolidation project in Saga, Japan

General description of the project

From June 2003 to March 2004, vacuum consolidation was carried out at a site in Saga, Japan, for a road construction project. The improved area was about 1 km long and 16–18 m wide. At the site, six boreholes and some piezocone tests were conducted to investigate the soil strata and mechanical properties of the deposit. Figure 2 shows the soil profiles revealed by the six boreholes (CEDSP 2004). In Fig. 2, fill refers to the sand mat constructed before boring. At the site, the thickness of the soft Ariake clay deposit (clay and silty clay layers in Fig. 2) is about 9–13 m. Ariake clay is a very soft clay deposit with a natural water content (w_n) generally in the range from 100% to 150% and compression index (C_c) of 1.5–2.5. For the purpose of field vac-

Fig. 2. Soil profiles at field test site.
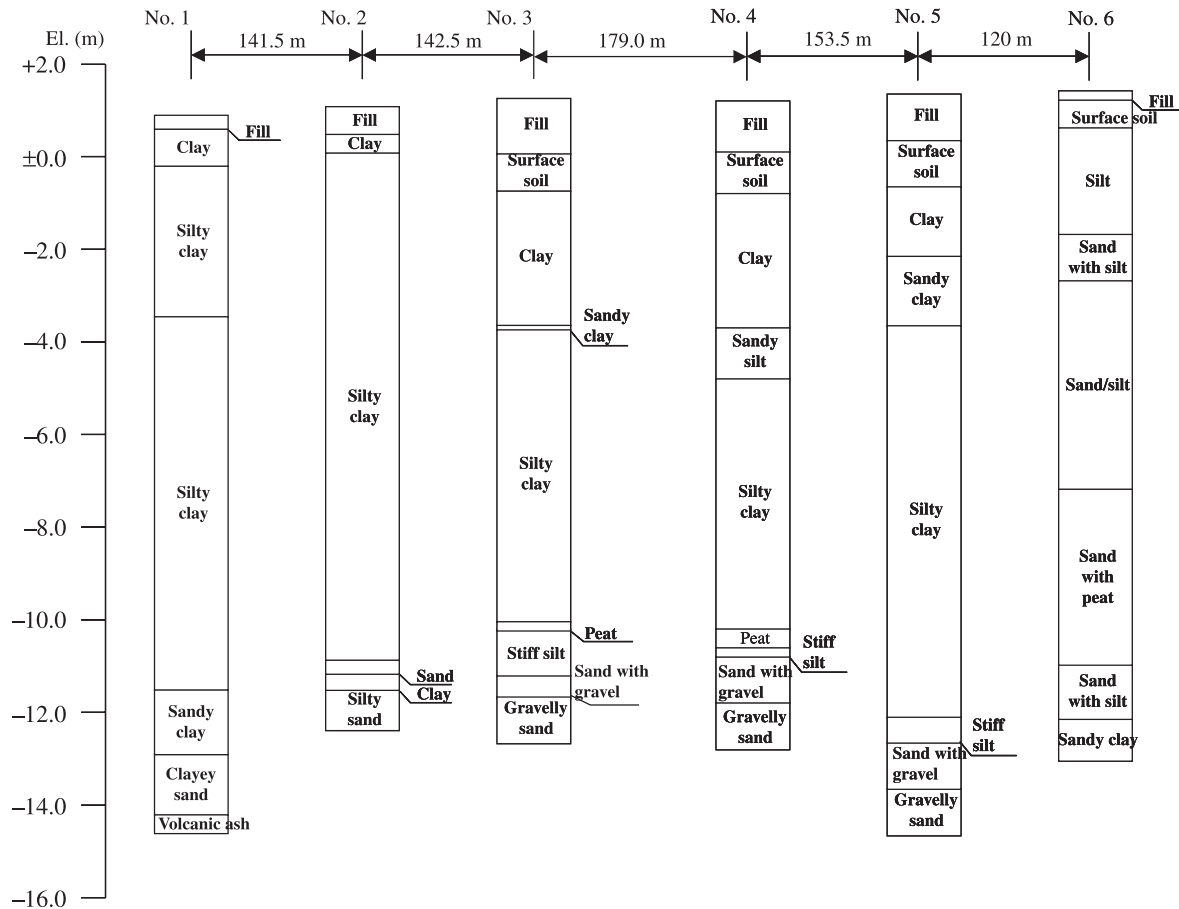
Fig. 3. Locations of test sections.
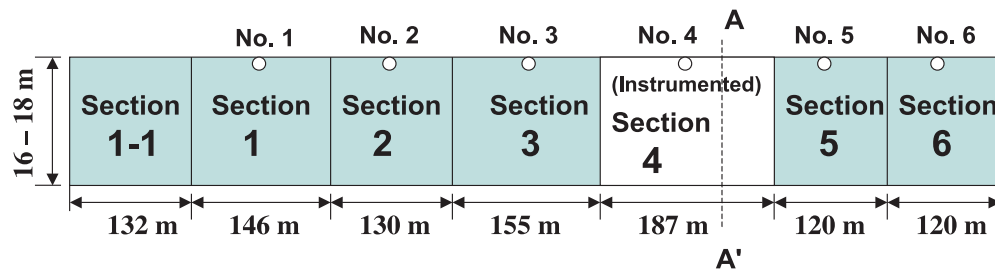
uum consolidation, the improved area was divided into seven sections (Fig. 3).

The air sealing sheet used for this project was a 0.5 mm thick polyvinyl chloride (PVC) membrane. Before the sealing sheet was placed, a sand mat about 1.0 m thick was placed on the ground surface to act as a drainage layer. PVDs were installed to a depth of 10.0–11.5 m from the top of the sand mat and arranged in a square pattern at 0.8 m spacing. In addition, prefabricated drains (0.3 m wide and 4.5 mm thick) were laid on top of the sand mat with a horizontal spacing of 0.8 m to ensure adequate horizontal drainage capacity. The groundwater level at the site was 0.5–1.5 m below the ground surface (1.0 m was assumed in subsequent analysis). To avoid air leakage through the top unsaturated zone, the edges of the sealing sheet were embedded in a 1.5 m deep trench.

Surface settlement and surface vacuum pressure gauges were installed in each test section. Section 4 had a relatively detailed instrumentation system around the line denoted A–A′ (see Fig. 3), as detailed later in the paper. Figure 4 shows the vacuum pressure variations and surface settlement curves for all sections. The vacuum pressure measured at the ground surface was generally within the range of 60–70 kPa, and the vacuum consolidation duration was about 80 days (except in section 1, where the duration was about 110 days). The measured surface settlement on the centreline of the improved area was 0.90–1.10 m except at location 2, where the settlement was about 0.55 m (CEDSP 2004). This is probably because the soil deposit at location 2 had been subjected previously to a surcharge load and was therefore stiffer than other test sections (CEDSP 2004). The starting time for application of vacuum consolidation of each

Fig. 4. Variations with time of vacuum pressure and surface settlement.
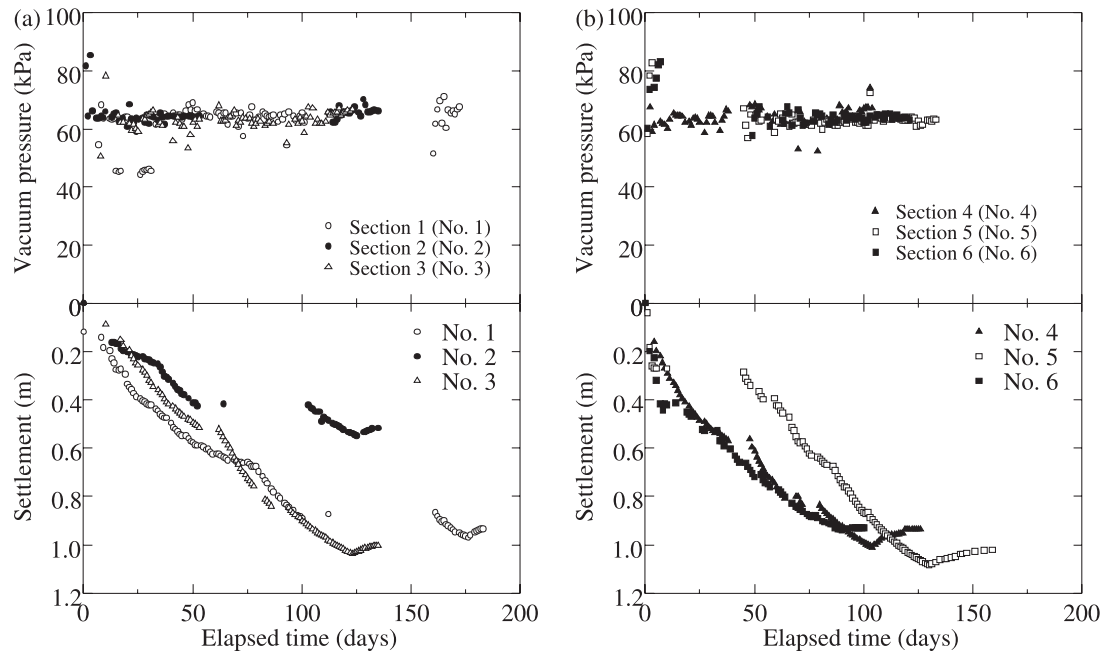
section was different; sections 5 and 6 were started in June 2003, sections 1 and 1-1 in September 2003, and sections 2, 3, and 4 in November 2003. Also, during the vacuum consolidation periods, there were temporary stops of the vacuum pumps.

Instrumentation and soil profile along line A–A′, section 4

For section 4, in addition to the surface settlement and the surface vacuum pressure gauges, subsurface settlement gauges (S-1, S-2, S-3), piezometers (P-1-1, P-1-2, P-1-3, P-2-1, P-2-2, P-3-1, P-3-2), and an inclinometer (I-1) were installed along and (or) around line A–A′, as illustrated in Figs. 5a and 5b.

Tanabashi et al. (2004) reported the soil profile and some index properties for the soil at the location of line A–A′, as indicated in Fig. 6. The liquid limits (w_l), plasticity limits (w_p), compression indices (C_c), maximum consolidation pressures (p_c), and hydraulic conductivities (k) of the soil layers were not reported, however. The values of these particular parameters given in Fig. 6 are from borehole 4, which was about 30 m from line A–A′ (Fig. 3). A piezocone sounding test was conducted along line A–A′ (see Fig. 5a for exact location), and the tip resistances (p_t) and pore-water pressures (u) from these piezocone tests are depicted in Fig. 7 (after Tanabashi et al. 2004). It can be seen that the soft layer was about 12.0 m thick (including the sand mat). The PVD installation depth was 11.5 m from the top of the sand mat or 10.5 m from the original ground surface.

At section 4, construction of the sand mat commenced on 20 May 2003, and vacuum consolidation was started on 20 November 2003. During construction of the sand mat, the settlement at S-1 (5.10 m below the top of the sand mat) was monitored. Just before the commencement of vacuum consolidation, the measured settlement at S-1 was 112 mm.

In this study, section 4 has been analyzed using the finite element method (FEM) for coupled consolidation. The pur-
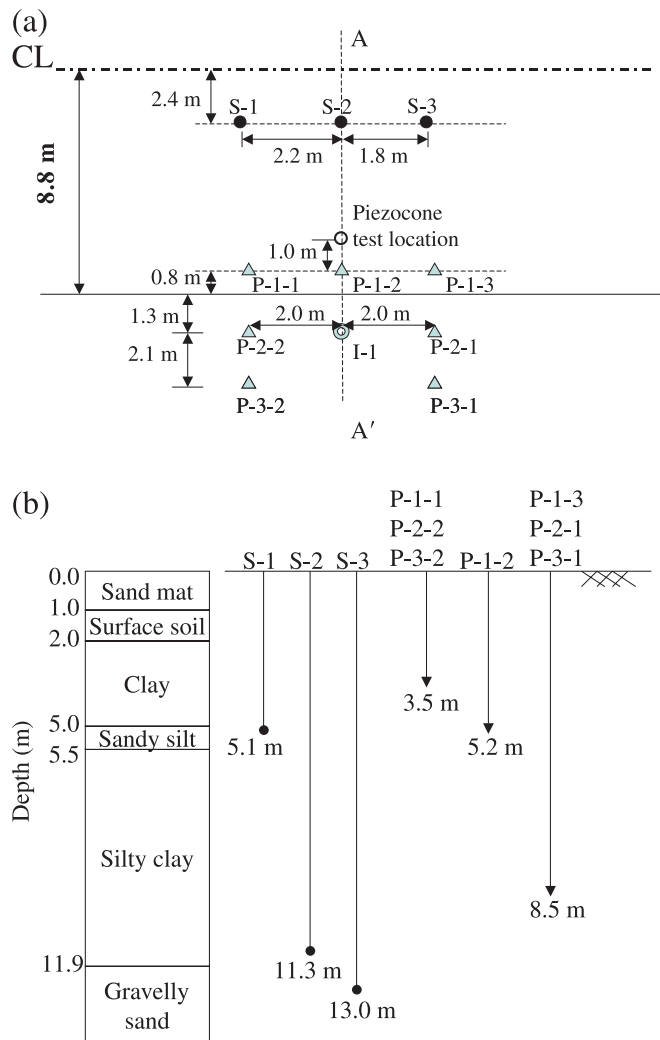
pose of the analysis was threefold: (i) calibrating the numerical procedure for simulating vacuum consolidation; (ii) investigating the effect of penetration depth of the prefabricated vertical drains (PVDs) for the case of two-way drainage of the subsoil subjected to vacuum consolidation; and (iii) studying the characteristics of the subsoil response when application of a vacuum pressure is combined with embankment loading.

FEM modeling

A coupled, Biot-type consolidation analysis was conducted assuming plane strain conditions of deformation and planar pore fluid flow. The finite element mesh and the mechanical and hydraulic boundary conditions adopted in this study are indicated in Fig. 8. In the FEM analyses, the behaviour of the clayey layers was represented by the modified Cam–Clay model (Roscoe and Burland 1968). The sand layers were treated as linear elastic materials (there is not enough information to warrant the adoption of a more sophisticated soil model). The adopted values of the soil parameters are given in Table 1. The values of λ, e_0, and γ_t were obtained directly from the laboratory test results (Fig. 6), κ values were calculated as $\lambda/10$, and ν and M values were assumed empirically. The values of hydraulic conductivity of Ariake clay deduced from laboratory consolidation test results normally underestimate the field values (Chai and Miura 1999). To obtain predictions of settlement with time that more closely match field observations, the assumed values of the vertical hydraulic conductivities (k_v), listed in Table 1, are twice the laboratory values given in Fig. 6. The horizontal values were assumed to be 1.5 times the corresponding vertical values (Chai and Miura 1999). During consolidation, the hydraulic conductivity was allowed to vary with voids ratio according to Taylor's equation (Taylor 1948):

[9] $\qquad k = k_0 10^{(e - e_0)/C_k}$

Fig. 5. Arrangement of instrumentation in section 4: (*a*) plan view of instrumentation points; (*b*) illustration of the depth of instrumentation points. CL, centreline.

and Miura 1999, 2002), and a case of vacuum pressure combined with embankment load on Bangkok clay (Bergado et al. 1998).

Measured and simulated performance at A–A′

At section 4, from 20 November to 27 December 2003, vacuum pumping was in operation only during the daytime, for 9 h per day. The field operation was also stopped during the New Year's holiday (28 December to 4 January). From 5 January 2004, the pump was operated for 24 h/day until the termination of the vacuum consolidation (on 1 March 2004). There was a break period from 31 January to 4 February 2004, however, due to some kind of mechanical problem (CEDSP 2004). In the field, only the steady vacuum pressure under the air sealing sheet was recorded during the day. There were no data available for the vacuum pressure variation when the pump was stopped after the 9 h/day operation period. As the pump was stopped at 17:00 PM, the vacuum pressure was recorded as approximately 60 kPa; at 09:00 AM the next morning, the remaining vacuum pressure had reduced to about 20–30 kPa (H. Inamata, field supervision engineer of the project, personal communication, 2005). Based on this information, the minimum vacuum pressure was assumed to be 20 kPa. Figure 9 gives the variation of the measured and simulated peak vacuum pressure applied daily at the surface, and Fig. 10 shows the assumed variation of the surface vacuum pressure during a single day accounting for the 9 h/day operation period. The field-measured data presented in the following sections are from Tanabashi et al. (2004, 2005) and CEDSP (2004).

Settlement

Figure 11 shows measured and simulated settlement–time curves. Generally, the analysis simulated the measured settlement curves well, but there are two significant discrepancies. First, the simulated rebounds are larger than the measured rebounds. This is considered to be due partly to the limitation of the adopted soil models and partly to some assumed parameters that may not represent the actual field values. Second, the simulated compression below 11.30 m (measured from the top of the sand mat) is less than those measured in the field. The reason for this discrepancy is that either the Young's modulus adopted for the layer of sand with gravel below the silty clay is too large or the boundary of the finite element mesh with vertical fixity (16 m from the top of the original ground surface) is too shallow. In Fig. 11, the contribution to the overall settlement arising from compression of the 1.0 m thick sand mat is excluded. The simulation included the sand mat construction process, however. It has been assumed that the construction time for the sand mat was 30 days, followed by a consolidation period of about 152 days before the commencement of vacuum consolidation. At the time of starting the vacuum consolidation, the simulated settlements at the ground surface and 5.10 m from the top of the sand mat (GL–5.10 m) were 168 and 95 mm, respectively. As explained previously, the corresponding measured settlement at GL–5.10 m was 112 mm, which is larger than the simulated value. Since the construction history for the sand mat was not recorded, the reported simulation is considered to be reasonable and further refinement unwarranted.

in which k_0 is the initial value of hydraulic conductivity (see Table 1 for assumed values); and the constant C_k was adopted as $0.5e_0$, where e_0 is the initial void ratio (Tavenas et al. 1986).

Values adopted for the parameters related to the behaviour of the PVDs are listed in Table 2 and have been selected following the recommendations of Chai and Miura (1999). In particular, the equivalent vertical hydraulic conductivity method (Chai et al. 2001) was adopted to model the PVD-improved subsoil. The initial stress state and the size of the initial yield locus adopted for the clayey and silty layers are listed in Table 3. A larger initial yielding locus was assigned for the surface crest layer so that it behaves initially as an overconsolidated soil.

The program used for these numerical analyses was CRISP-AIT (Chai 1992), which was modified from the original program CRISP (Britto and Gunn 1987). Using similar means for determining model parameters, the same program has been used to successfully simulate the behaviour of embankments on the Muar clay deposit, Malaysia, and the Ariake clay deposit, Japan (Chai and Bergado 1993; Chai

Fig. 6. Soil profile and some index and mechanical properties (data from Tanabashi et al. 2004; CEDSP 2004).
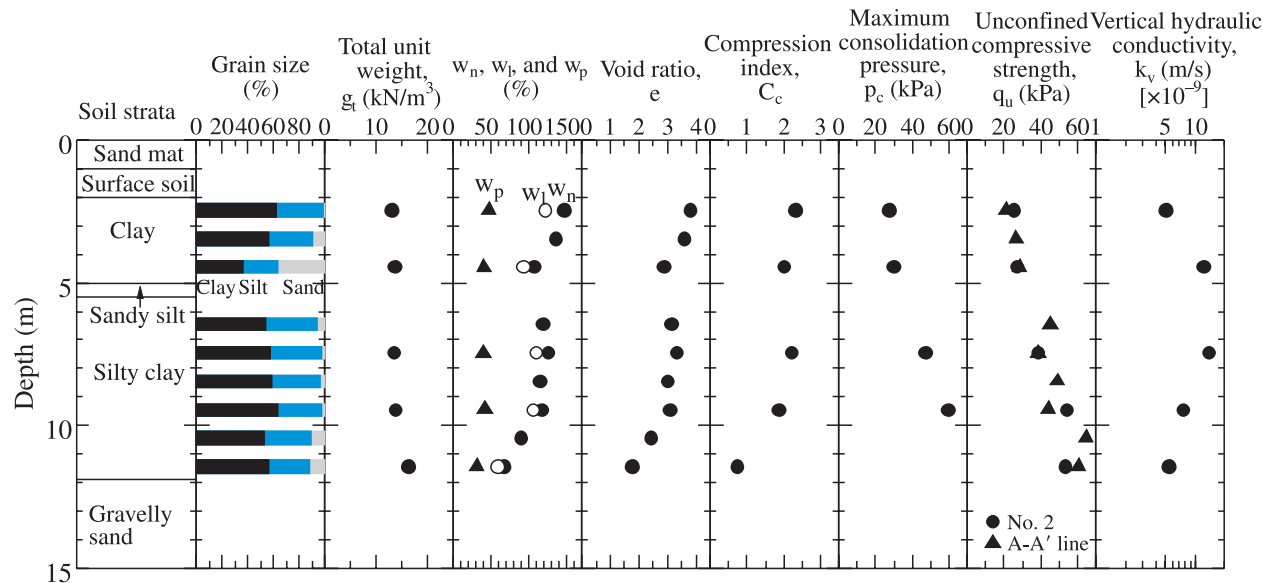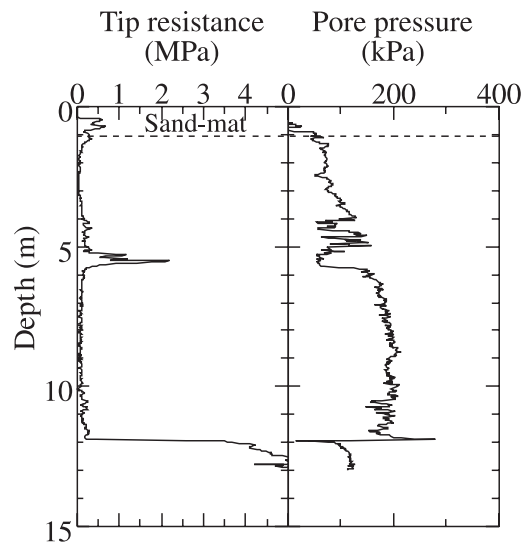

Fig. 7. Piezocone test results (after Tanabashi et al. 2004).

The simulated and measured ground surface settlement profiles at the end of the vacuum consolidation (when the pumps are switched off) are compared in Fig. 12. The FEM analysis yielded results that are generally acceptable, except at the location about 4.2 m away from the edge of the area treated by vacuum consolidation, where the simulated settlements are less than the measured settlements. The reasons for this discrepancy are not yet clear, but perhaps the value adopted for the horizontal hydraulic conductivity of the sandy silt layer located about 5.0 m below the top of the sand mat is less than the actual field value. As shown in Fig. 8, it was assumed that at the right-hand boundary, this sandy silt layer is fully drained. The presence of this layer provides a preferred horizontal drainage pathway, and the vacuum pressures will therefore progress laterally through this layer over time. The higher the hydraulic conductivity of the layer, then the faster will be this progression. Faster lateral transfer of the suction pressures would result in more

settlement beyond the edge of the treated area at the time when the vacuum pumping ceases. Comparing the simulated and measured pore-water pressures at about 1.3 and 3.5 m away from the edge of the vacuum consolidation improved area (Figs. 14a, 14b), however, does not support this argument.

Lateral displacement

Figure 13 depicts the lateral displacements induced by vacuum consolidation at the inclinometer location (see Fig. 5a). It can be seen that, except at the ground surface, the simulation underestimated the inward lateral displacement. To yield a larger inward lateral displacement from the FEM analysis, the size of yield loci in Table 3 for the upper soft layer (0–5.0 m depth) would need to be reduced. Such adjustment is not supported by the test data given in Fig. 6, however, and would result in a larger predicted settlement than the field measurement. This discrepancy may due to the inability of the constitutive model and (or) numerical techniques adopted to simulate the deformation response of the deposit under vacuum pressure (particularly if the real soil is anisotropic). Although not confirmed (all theories for PVD consolidation ignore the effect of lateral displacement), another possible reason is that using an equivalent hydraulic conductivity in the vertical direction to simulate the effect of PVDs may underestimate the lateral displacement. In addition, when measuring lateral displacement using an inclinometer, there is a possible problem of stiffness compatibility between the inclinometer casing and the surrounding soft subsoil. If the casing is stiffer than the soil, there is the possibility of relative movement between the casing and the soil. In such an event the inclinometer reading would give a false impression of the actual lateral movement of the soil.

Pore-water pressure

Figure 14 shows a comparison of the measured and simulated variations in total pore-water pressure. Since measurement at the piezometer points P-1-1, P-1-2, and P-1-3

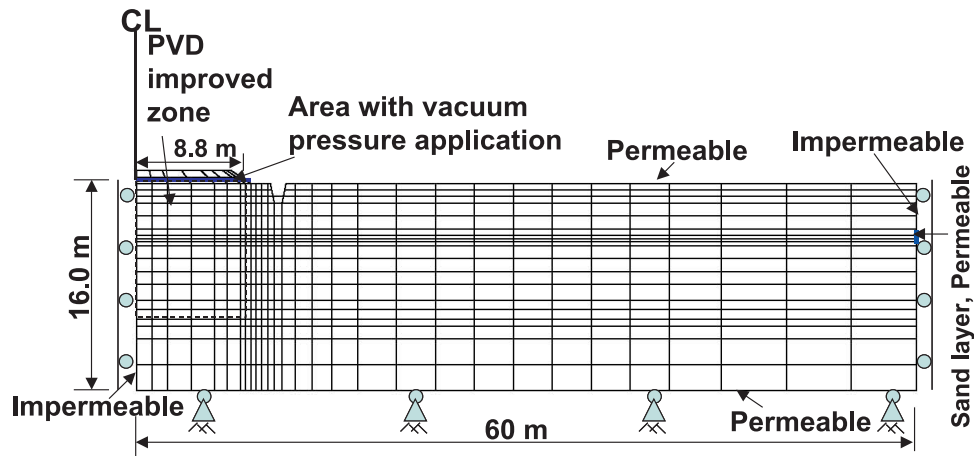**Fig. 8.** FEM mesh and boundary conditions.

Table 1. Soil parameters for finite element analysis.

Depth (m)	Soil	E (kPa)	ν	κ	λ	M	e_0	γ_t (kN/m³)	k_h ($\times 10^{-8}$ m/s)	k_v ($\times 10^{-8}$ m/s)
Fill		10 000	0.25	—	—	—	—	18.0	—	—
0.0–1.0	Surface layer	—	0.30	0.10	1.00	1.2	3.8	13.3	1.52	1.02
1.0–4.0	Clay	—	0.30	0.08	0.87	1.2	3.2	13.7	3.69	2.46
4.0–4.5	Sandy silt	—	0.30	0.03	0.30	1.2	2.0	15.5	29.00	29.00
4.5–9.0	Silty clay 1	—	0.25	0.09	0.89	1.2	3.0	13.8	290.00	2.32
9.0–11.0	Silty clay 2	—	0.30	0.03	0.30	1.2	1.6	16.3	1.65	1.10
11.0+	Gravelly sand	20 000	0.25	—	—	—	—	18.0	290.00	290.00

Note: e_0, initial void ratio; E, Young's modulus; k_h, hydraulic conductivity in horizontal direction; k_v, hydraulic conductivity in vertical direction; M, slope of critical state line in q–p' plot (where q is deviator stress and p' is mean effective stress); γ_t, unit weight; κ, slope of unloading–reloading line in e–lnp' plot; λ, slope of consolidation line in e–lnp' plot; ν, Poisson's ratio.

Table 2. Drain parameters.

| Parameter	Value
Unit cell diameter, D_e (m)	0.90
Drain diameter, d_w (mm)	52.3
Smear zone diameter, d_s (m)	0.3
Discharge capacity, q_w (m³/day)	0.27
Hydraulic conductivity ratio, k_h/k_s	10

Note: k_s, hydraulic conductivity of smear zone.

Table 3. Initial stress in the subsoil.

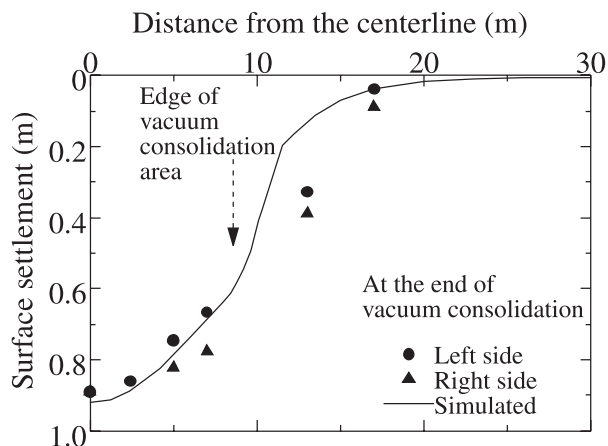| Depth (m)	σ'_{h0} (kPa)	σ'_{v0} (kPa)	Size of yield locus, p'_y (kPa)
0	5.0	0.0	51.0
1.0	9.7	13.8	51.0
1.5	9.5	15.8	37.1
2.0	10.6	17.7	34.5
2.5	9.8	19.7	31.9
4.0	12.8	25.5	30.7
4.5	14.2	28.4	34.2
9.0	23.2	46.4	55.9
11.0	29.7	59.4	71.5

Note: σ'_{h0} and σ'_{v0}, effective initial horizontal and vertical pressure, respectively.

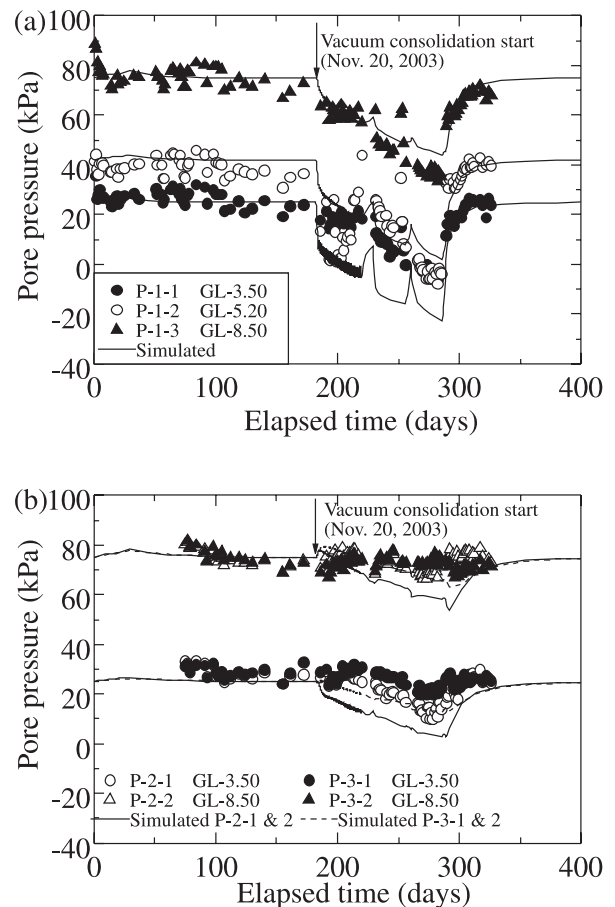**Fig. 9.** Measured and simulated peak vacuum pressure.
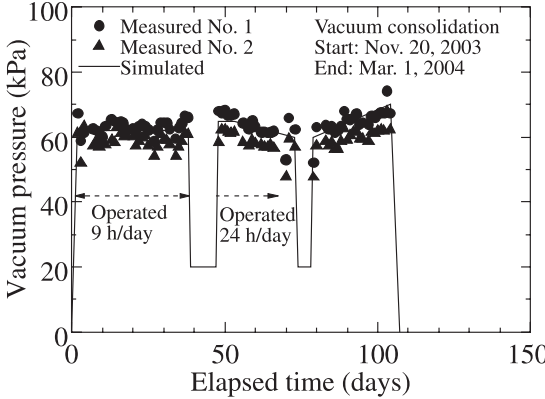
commenced at the beginning of the sand mat construction, the comparisons also commence at that time. For the purpose of calculating the total pore-water pressures, it was assumed that the groundwater table remained at the level of the original ground surface during the entire period of ground treatment. Observations of groundwater levels made prior to the vacuum treatment certainly indicate that the water table was generally at or just below the original ground surface, supporting the adoption of this assumption. It is noted, however, that this particular assumption is at slight

Fig. 10. Simulated vacuum pressure variation during daily operation.
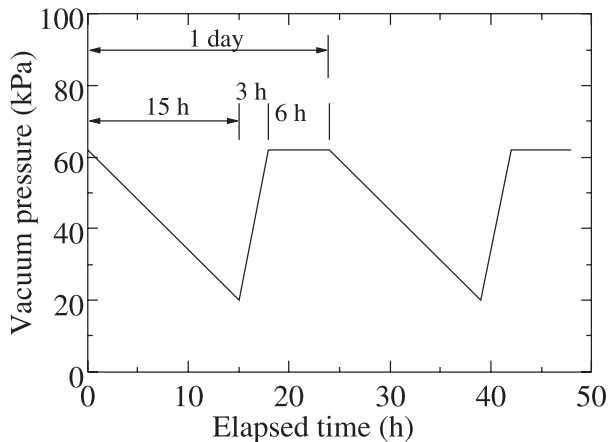
Fig. 11. Comparison of measured and simulated settlements.
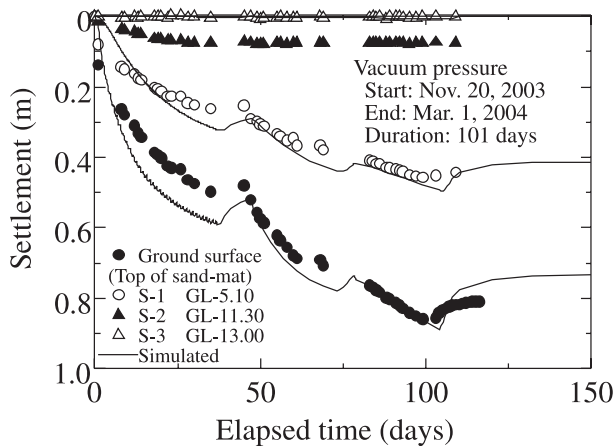
Fig. 12. Surface settlement profile.

Fig. 13. Comparison of measured and simulated lateral displacement.
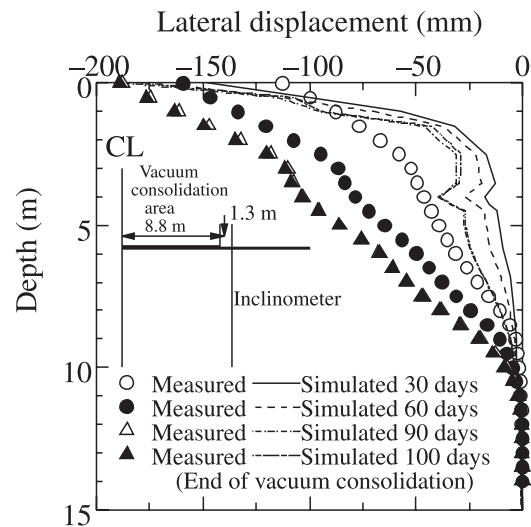
Fig. 14. Comparisons of pore-water pressure variations: (*a*) at P-1-1, P-1-2, and P-1-3; (*b*) at P-2-1, P-2-2, P-3-1, and P-3-2.

variance with another assumption made in the numerical model when estimating the initial state of effective stress in the ground. As mentioned previously, for estimating the initial effective stresses the groundwater level was assumed to be 1.0 m below the original ground surface. With an elastoplastic soil model, the stiffness and strength of a soil deposit depend on the effective stress in the deposit. There-

fore, the groundwater level used for calculating the initial effective stress not only represents the groundwater level measured at a particular period, but also reflects the mean groundwater level in the past. Although during the period of

the project there might have been some variation in the groundwater level, and given the simplifying assumptions that were made when predicting water pressures, overall the comparison between the measured and simulated pore-water pressures is good. Figure 14*a* shows that the simulated maximum drawdown of pore-water pressure was less than the measurements at GL–8.50 m and GL–5.20 m and greater than the measurement at GL–3.50 m. Figure 14*b* shows that the simulated pore-water pressure drawdown at P-2-1 and P-2-2 (1.3 m away from the edge of the improved area) was greater than the corresponding measurement.

The comparisons of predictions and field measurements presented here indicate that, although the adopted numerical technique simulated the lateral displacements of the subsoil only qualitatively well, it was able to simulate well, both qualitatively and quantitatively, the settlements and pore-water pressures under and (or) around the area treated with vacuum consolidation. It is generally considered that for most practical purposes the numerical technique adopted is capable of adequately simulating the response of the soil deposit subjected to vacuum pressure treatment.

Further simulation

Effect of PVD penetration depth

Given the values of soil parameters adopted for the Saga soils, an optimum PVD penetration depth of about 9.3 m (measured from the original ground surface) can be obtained from eqs. [5]–[8]. In estimating this optimum penetration depth, the effect of the sand layer at 5.0–5.5 m from the ground surface is ignored. This depth of penetration can be compared with the actual value of 10.5 m used at the Saga test site, which was also the value used in the foregoing finite element analyses. FEM analyses with PVD penetration depths of 9.0 and 9.7 m (measured from the original ground surface), which bracket the optimum penetration depth, were also conducted to provide an indication of the effects of penetration depth on the response of ground treated by vacuum consolidation. During these analyses, all other conditions were kept the same as in the previous analyses of the Saga test site.

The predicted surface settlements at the centre of the vacuum consolidation area are compared in Fig. 15. It can be seen that the case with 9.0 m PVD penetration depth exhibits greater settlement (slightly greater than the case of 9.7 m PVD penetration depth). A penetration depth of 9.0 m is less than the estimated "optimum" value of 9.3 m. A depth of 9.0 m, however, is at a boundary of changing compressibility of the soil layers, and as mentioned previously the proposed method may not provide the optimum depth (corresponding to maximum settlement) in such situations. In terms of settlement, an increase of the vacuum pressure is more effective above 9.0 m depth than below 9.0 m. Figure 16 shows the simulated vacuum pressure distribution with depth at the end of vacuum consolidation. The area enclosed by the vertical axis (on the right-hand side of the figure) and the vacuum pressure distribution curve for a PVD penetration depth of 9.7 m is slightly larger than the area corresponding to the case of 9.0 m penetration. The soil layers above 9.0 m depth are more compressible than those below 9.0 m depth, however, and as a result the settlement predicted for the 9.0 m

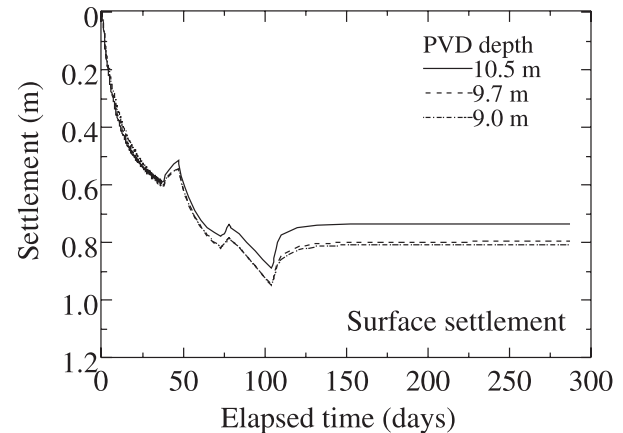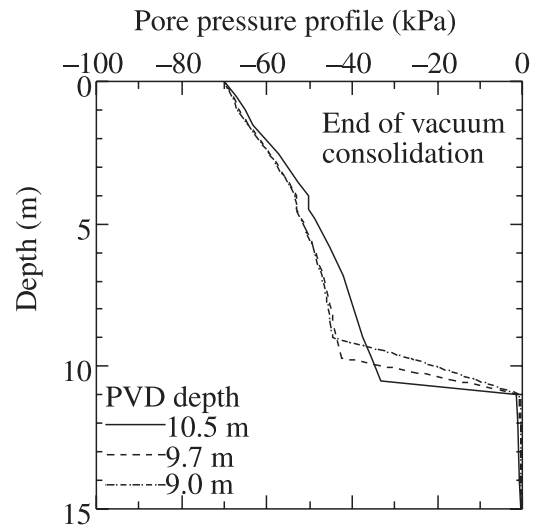**Fig. 15.** Effect of PVD installation depth on surface settlement.

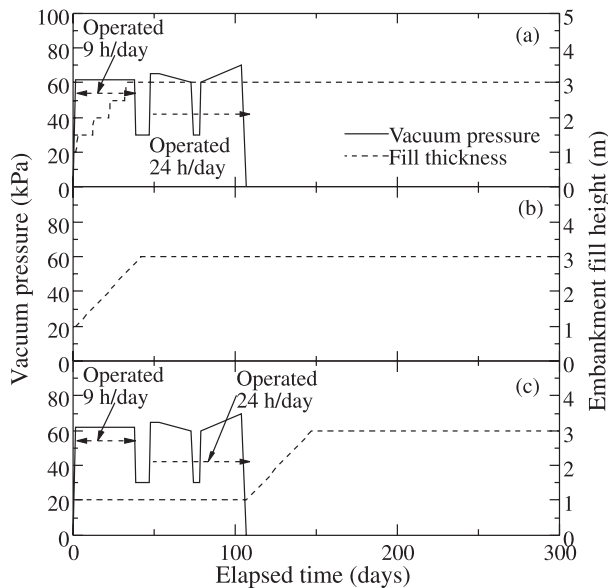**Fig. 16.** Vacuum pressure distribution with depth.

case is slightly greater than that predicted for the 9.7 m case. Nevertheless, these analyses indicate (*i*) the actual PVD improvement depth of 10.5 m was not optimum, being too deep for the most economic choice; and (*ii*) the PVD penetration depth estimated by the method proposed in this study provides a useful reference for the design of vacuum consolidation treatment using PVD improvement in the case of soil deposits with two-way drainage.

### Combination of vacuum pressure with embankment loading

To investigate the subsoil response when vacuum pressure treatment and embankment preloading are combined, the following three hypothetical cases were analyzed: (1) combining vacuum pressure and embankment preloading; (2) embankment preloading only; and (3) constructing an embankment on the improved subsoil after vacuum consolidation.

The assumed vacuum pressure and fill thickness variations for each case are given in Fig. 17. The assumed vacuum pressure variation is the same as that at section 4 of the field test in Saga, Japan. It was assumed that the total thickness of the embankment fill was 3.0 m, with a 1.0 m thick sand mat

Fig. 17. Assumed variations of vacuum pressure and embankment thickness: (*a*) case 1; (*b*) case 2; (*c*) case 3.
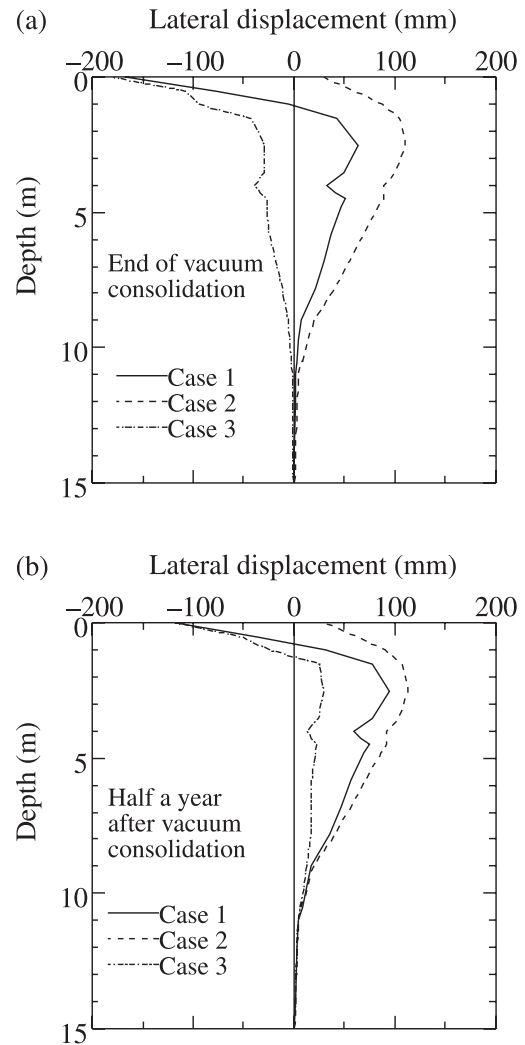

Fig. 18. Comparison of surface settlements.

Fig. 19. Comparison of lateral displacements: (*a*) at end of vacuum consolidation; (*b*) half a year after vacuum consolidation.
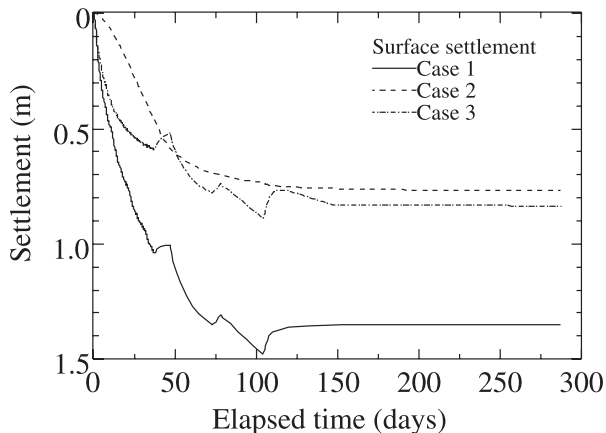
constructed before vacuum consolidation and the remaining 2.0 m thick fill constructed at an average rate of 50 mm/day.

Figure 18 compares calculated settlement curves at the centre of the treated region. It can be seen that combining embankment loading with vacuum pressure treatment (case 1) results in more settlement than in the other two cases, with about 1.75 times the predicted final settlement for the case of only an embankment preload (case 2) and about 1.60 times the predicted final settlement for the case of first consolidating under a vacuum pressure and then constructing the embankment (case 3). For case 1, after release of the vacuum pressure (about 65 kPa) the soft clayey layer is in an overconsolidated state, with an overconsolidation ratio (OCR) of about 2.0. For case 2, the subsoil is in a normally consolidated state, with an applied surface consolidation pressure of about 54 kPa. For case 3, after release of the vacuum pressure a 2.0 m thick embankment load was applied (corresponding to an applied vertical loading of about 36 kPa) and the subsoil is in a lightly overconsolidated state. For a road constructed on overconsolidated subsoil, there will be less traffic-load-

induced settlement and consequently lower ongoing maintenance costs.

Comparisons of the predicted lateral displacement profiles at the end of vacuum consolidation and half a year after vacuum consolidation are given in Figs. 19*a* and 19*b*, respectively. The lateral displacement induced by the sand mat loading is not included in the displacements plotted in Fig. 19. Case 3 has the smallest and case 2 has the largest lateral displacements. Comparing cases 1 and 2 indicates that the vacuum pressure treatment reduced the maximum lateral displacement by about 48 mm at the end of the vacuum consolidation and by about 20 mm half a year after the vacuum consolidation. With the release of vacuum pressure, there was some increase in lateral displacement. Although the numerical technique adopted in this study underestimates the lateral displacement of the field vacuum consolidation project at Saga, Japan, it is believed that qualitatively the comparison given in this section is valid.

Conclusions

The response of a soft clayey deposit to vacuum consolidation treatment has been discussed and investigated by the

finite element method (FEM). Specific reference has been made to a vacuum consolidation project conducted in Saga, Japan. The following conclusions are drawn based on the results presented here.

(1) Prefabricated vertical drain (PVD) penetration depth — In cases of two-way drainage of soft clayey deposits (e.g., where a sand or gravel layer underlies the clayey layer), when combining the use of PVDs with vacuum consolidation, the PVDs should not penetrate the entire clayey layer to avoid vacuum pressure loses in the underlying sand or gravel layer. An equation for calculating the optimum penetration depth of PVDs has been proposed.

(2) Advantages of combining vacuum pressure with embankment load — This combination can increase the overall effective surcharge load, substantially reduce or limit the preloading induced lateral displacement of the subsoil, and allow shorter construction times, especially for road construction.

(3) Analysis of a field test involving vacuum consolidation at Saga, Japan — A vacuum consolidation project conducted in Saga, Japan, was analyzed using a plane strain finite element method for coupled consolidation. The analyses simulated very well the settlements and porewater pressures but simulated only moderately well the lateral ground displacements. Overall it was shown that the numerical techniques adopted can simulate reasonably well the response of the subsoil under vacuum pressure.

(4) Numerical investigations of subsoil response to vacuum consolidation — Adopting the field conditions at the vacuum consolidation test site in Saga, Japan, to be specific, numerical investigations were subsequently conducted for the cases of different PVD penetration depths and various combinations of vacuum pressure with embankment loading. The numerical results confirmed the usefulness of the method proposed for determining the optimum PVD penetration depth in the case of a two-way drainage deposit under vacuum consolidation and demonstrated the advantages of combining vacuum pressure with embankment loading.

References

Bergado, D.T., Chai, J.-C., Miura, N., and Balasubramaniam, A.S. 1998. PVD improvement of soft Bangkok clay with combined vacuum and reduced sand embankment preloading. Geotechnical Engineering Journal, Southeast Asian Geotechnical Society, **29**(1): 95–121.

Britto, A.M., and Gunn, M.J. 1987. Critical state soil mechanics via finite elements. Ellis Horwood Limited, Chichester, UK. 486 pp.

CEDSP. 2004. Site investigation report, ground improvement project, Kohoku-Ashikari Road. Civil Engineering Department, Saga Prefecture (CEDSP), Saga, Japan.

Chai, J.-C. 1992. Interaction between grid reinforcement and cohesive–frictional soil and performance of reinforced wall/embankment on soft ground. Ph.D. dissertation, Asian Institute of Technology, Bangkok, Thailand.

Chai, J.-C., and Bergado, D.T. 1993. Performance of reinforced embankment on Muar clay deposit. Soils and Foundations, **33**(4): 1–17.

Chai, J.-C., and Miura, N. 1999. Investigation of some factors affecting vertical drain behavior. Journal of Geotechnical and Geoenvironmental Engineering, ASCE, **125**(3): 216–226.

Chai, J.-C., and Miura, N. 2002. Traffic load induced permanent deformation of road on soft subsoil. Journal of Geotechnical and Geoenvironmental Engineering, ASCE, **128**(11): 907–916.

Chai, J.-C., Shen, S.-L., Miura, N., and Bergado, D.T. 2001. Simple method of modeling PVD improved subsoil. Journal of Geotechnical and Geoenvironmental Engineering, ASCE, **127**(11): 965–972.

Chai, J.-C., Hayashi, S., and Carter, J.P. 2005a. Characteristics of vacuum consolidation. In Proceedings of the 16th International Conference on Soil Mechanics and Geotechnical Engineering, Osaka, Japan, 12–16 September 2005. Mill Press, Rotterdam, The Netherlands. Vol. 3, pp. 1167–1170.

Chai, J.-C., Carter, J.P., and Hayashi, S. 2005b. Ground deformation induced by vacuum consolidation. Journal of Geotechnical and Geoenvironmental Engineering, ASCE, **131**(12): 1552–1561.

Hansbo, S. 1981. Consolidation of fine-grained soils by prefabricated drains. In Proceedings of the 10th International Conference on Soil Mechanics and Foundation Engineering, Stockholm, 5–19 June 1981. A.A. Balkema, Rotterdam, The Netherlands. Vol. 3, pp. 677–682.

Kjellman, W. 1952. Consolidation of clayey soils by atmospheric pressure. In Proceedings of the Conference on Soil Stabilization, Boston, Mass., June 1952. Massachusetts Institute of Technology, Cambridge, Mass. pp. 258–263.

Roscoe, K.H., and Burland, J.B. 1968. On the generalized stress–strain behavior of 'wet' clay. In Engineering plasticity. Edited by J. Heyman and F.A. Leckie. Cambridge University Press. pp. 535–609.

Tanabashi, Y., Jiang, Y., Mihara, H., Li, B., Uehara, T., Shiono, T., and Saitou, F. 2004. Field investigation and model test for clarifying compaction effect of CVC (compact vacuum consolidation) method. In Proceedings of the Vietnam–Japan Joint Seminar on Geotechnics and Geoenvironent Engineering, Hanoi, November 2004. Vietnam Soil Mechanics and Geotechnical Engineering Society, Hanoi, Vietnam. pp. 27–32.

Tanabashi, Y., Shiono, T., Mihara, H., and Jiang, Y. 2005. Investigation of consolidation promoting method by field and model tests for vacuum consolidation method. Journal of Civil Structure and Material, **21**: 97–104. [In Japanese.]

Tang, M., and Shang, J.Q. 2000. Vacuum preloading consolidation of Yaogiang Airport runway. Géotechique, **50**(6): 613–623.

Tavenas, F., Tremblay, M., Larouche, G., and Leroueil, S. 1986. In situ measurement of permeability in soft clays. In Use of In Situ Testing in Geotechnical Engineering: Proceedings of the ASCE Specialty Conference, Blacksburg, Va. Edited by S.P. Clemence. Geotechnical Special Publication 6, ASCE, Reston, Va. pp. 1034–1048.

Taylor, D.W. 1948. Fundamentals of soil mechanics. John Wiley & Sons Inc., New York.

Tran, T.A., Mitachi, T., and Yamazoe, N. 2004. 2D finite element analysis of soft ground improvement by vacuum-embankment preloading. In Proceedings of the 44th Annual Conference of Hokkaido Branch, Japanese Geotechnical Society, February 2004, Sapporo, Japan. pp. 127–132.